Wave Motion 48 (2011) 275–289

Contents lists available at ScienceDirect

Wave Motion

journal homepage: www.elsevier.com/locate/wavemoti

The far-field scattering response of a side drilled hole in single/layered anisotropic media in ultrasonic pulse-echo setup

Jing Ye [a,1], Hak-Joon Kim [a,1], Sung-Jin Song [a,*], Sung-Sik Kang [b], Kyungcho Kim [b], Myung-Ho Song [b]

[a] School of Mechanical Engineering, Sungkyunkwan University, 300 Chunchun-dong, Jangan-gu 440-746, Republic of Korea
[b] Korea Institute of Nuclear Safety, Daejeon 305-338, Republic of Korea

ARTICLE INFO

Article history:
Received 23 August 2010
Received in revised form 11 November 2010
Accepted 15 November 2010
Available online 24 November 2010

Keywords:
Ultrasonic
Scattering
Side drilled hole
Anisotropic media

ABSTRACT

Ultrasonic testing for defects in anisotropic material is one of the difficult problems in non-destructive testing (NDT) with elastic waves. Even though a series of studies have been performed on the waves interacting with flaws, however, only a small portion was on anisotropic materials. In this paper, an analytical solution for the far-field scattering response of a side drilled hole (SDH) in anisotropic media in an ultrasonic pulse-echo setup with its incident wave normal to the axis of cylindrical hole is presented. The solution is based on the Kirchhoff approximation, and validated upon several numerical examples, yielding satisfactory results in the comparison to the results achieved by different methods. Also, an attempt is made to extend the use of this solution from homogeneous anisotropic media to weld, which is considered as the multi-layer anisotropic media.

1. Introduction

Ultrasonic nondestructive testing for defects is a common testing procedure in aerospace industries, nuclear power industries, etc., where the main task is to identify locations of anomalies and their quantification in order to assess their lifetime. As the properties of the composite materials and welds allow the significant improvements in the performances of aircrafts and power plants, the demand of such materials is increasing rapidly. Thus, to get a deeper understanding of the testing in such materials and how waves scatter from various types of flaws, theoretical predictions for the scattering response of a flaw in the anisotropic media are very valuable. Moreover, it is valuable to improve the efficiency of the calculation of the wave propagation in such a complex material.

In the ultrasonic nondestructive testing, side drilled hole (SDH) is one of the major standard reflectors which are used for the calibration of equipments and transducers. The SDH is drilled parallel to the scanning surface and presents the same reflector to all beam angles. A single calibration block containing several SDHs at different depths can therefore be used to generate a distance amplitude correction (DAC) curve for any probe. Many authors have studied the measurement models and scattering models for predicting the ultrasonic pulse-echo response from the SDH using different approaches. For the measurement models, Lopez-Sanchez et al. [1] developed two reciprocity-based measurement models to predict the ultrasonic response from an SDH, one suitable for large SDHs and one for small SDHs and the simulation results were compared with the experimental ones. For the scattering models, an analytical method like the separation of variables was studied by White [2], Niklasson and Datta [3]. Krautkrämer and Krautkrämer [4] used simple high-frequency arguments to investigate the scattering dependence on the frequency and SDH radius. Chapman [5] used an analytical approximation in conjunction with a simple model of an ultrasonic probe to determine the scattering by an SDH and employed this for calibration, see also Schmerr [6]. Bostrom and Bovik adopted the T matrix solution [7]. However, these were applied in the isotropic or transversely isotropic materials only. Purely numerical

* Corresponding author. Tel.: +82 31 290 7493.
E-mail addresses: yejing@skku.edu (J. Ye), hjkimc21@skku.edu (H.-J. Kim), sjsong@skku.edu (S.-J. Song).
[1] Tel.: +82 31 290 7493.

0165-2125/$ – see front matter
doi:10.1016/j.wavemoti.2010.11.003

methods, like the finite element method (FEM) and the elastodynamic finite integration technique (EFIT), which can handle the anisotropic inhomogeneous media in the three dimensions were studied by Harumi et al. [8] and Fellinger et al. [9]. But as the number of degrees of freedom becomes too large in 3D in the anisotropic materials, a personal computer was not able to afford to calculate the scattering problems. Nowadays, the semi-analytical technique is gaining more and more popularity in the field of ultrasonic wave propagation. The Distributed Point Source Method (DPSM) developed by Placko and Kundu [10] has been used to model the elastic wave scattering in a homogeneous solid half-space with a circular cylindrical hole [11]. This mesh-free semi-analytical technique circumvents the problem of small mesh size requirements and works well at high frequencies. Another analytical approximation, the Kirchhoff approximation also called the tangent-plane method, is a very versatile approximation. It is assumed in this approximation that on the part of the flaw surface where the incident wave can directly strike, the interaction of the incident wave with the surface is identical to that of an incident plane wave with a plane interface whose normal coincides locally with the flaw surface normal. On the remainder of the flaw surface, the elastic wave fields are assumed to be zero. Using this approximation, the analytical solutions for arbitrary boundaries and volumes can be derived. Additionally, the computation time is minimized since no matrix inversion is involved. It extends well beyond the size/frequency and angular ranges commonly assumed for this approximation. Besides, it can accurately predict the very early response of the flaw in isotropic media to a very wide range of cases [12].

Spies has applied the Kirchhoff approximation for the circular shape defects embedded in an anisotropic material [13]. Huang et al. have obtained an analytical expression for the pulse-echo leading edge response of an arbitrary volumetric flaw in an anisotropic medium and pitch–catch response of a flat elliptical crack [14]. To our knowledge, so far there's no paper published on the scattering behavior of an SDH in anisotropic material. This study presents a derivation of the expression for the pulse-echo response of an SDH embedded in an anisotropic medium.

In the following sections, the analytical solution of the far-field scattering response of an SDH in the anisotropic media in the ultrasonic pulse-echo setup is derived. First, we will outline the measurement model for SDH. Then we demonstrate how the Kirchhoff approximation is adopted to obtain the analytical solution. At the end of the section, the reflection coefficients for a plane interface are derived for the numerical integral. In Section 3, the numerical results in the frequency domain and time domain are presented in both one medium and two layered media in order to explore the application of this model to weld, which is considered as the multi-layered anisotropic materials. Section 4 is devoted to conclusion.

2. Analytical solution for the far-field scattering response of an SDH in anisotropic media in the ultrasonic pulse-echo setup

2.1. A measurement model for SDH

The measurement model for SDH has been already discussed in detail by Schmerr et al. [6,12], and Lopez-Sanchez [1], therefore only the basic equations of the measurement model of the SDH have been given here for the continuity of our discussion. The modeling of the ultrasonic NDE inspections for the SDH is a rather complex problem, which involves the radiation, propagation, scattering by a flaw and reception of ultrasonic waves. Fortunately, this complex problem can be handled using a measurement model based on the reciprocity relationship, which were introduced by Auld in 1979 [15]. In the relationship, the voltage response $V_R(\omega)$ at the angular frequency ω received by a transducer in the absence (state 1) and in the presence of a flaw (state 2) was related to the elastodynamic field taken in both states integrated on a surface, S_f, of the flaw, which can be written as:

$$V_R(\omega) = \frac{s(\omega)}{v_T v_R Z_r^{T;a}} \int_{S_f} \left[\tau_{ij}^{(1)}(\mathbf{x},\omega) v_i^{(2)}(\mathbf{x},\omega) - \tau_{ij}^{(2)}(\mathbf{x},\omega) v_i^{(1)}(\mathbf{x},\omega)\right] n_i(\mathbf{x}) dS(\mathbf{x}) \tag{1}$$

where the system function $s(\omega)$ combines the effects of the pulser/receiver, cabling and the transducer on the measured signals, v_T and v_R are the average velocities on the face of the receiving and the transmitting transducers respectively. The fields $\tau_{ij}^{(1,2)}$ and $v_i^{(1,2)}$ are the stress field and the particle velocity obtained in states 1 and 2. The quantity $Z_r^{T;a}$ is an acoustic impedance of the transmitting transducer and n_i is the component unit outward normal to the flaw.

Assuming the incident wave fields are quasi plane waves of the wave type α, then for state 1, the total velocity field and stress field can be written as:

$$v_i^{(1)} = v_0 \hat{V}^\alpha d_i^\alpha \exp(ik_a \mathbf{e}^\alpha \cdot \mathbf{x}) \tag{2}$$

$$\tau_{ij}^{(1)} = -\frac{v_0}{c_\alpha} \hat{V}^\alpha C_{ijkl} d_k^\alpha e_l^\alpha \exp(ik_a \mathbf{e}^\alpha \cdot \mathbf{x}) \tag{3}$$

where c_α and k_α are the wave speed and wave number of the incident wave of type α in the solid. And $\hat{V}^\alpha$, the velocity amplitude of the incident wave at a point $\mathbf{x}$, is normalized by the velocity amplitude v_0 at the transducer's surface. The term C_{ijkl} is the stiffness tensor for the solid. The unit vector $\mathbf{e}^\alpha$ is a unit vector of the phase velocity of the incident wave, while d_i^α is the polarization of the incident wave.

For state 2, the total velocity field and stress field including incident wave and scattered wave can be given by expressions similar to Eqs. (2) and (3), if the reflected wave type is m, as follows:

$$v_i^{(2)} = \frac{v_0 \hat{V}^m}{-i\omega} \tilde{v}_i \tag{4}$$

$$\tau_{ij}^{(2)} = \frac{\tau_0 \hat{V}^m}{-i\omega} \tilde{\tau}_{ij} \tag{5}$$

where $\tilde{v}_i$ and $\tilde{\tau}_{ij}$ are the dimensionless quantities representing the normalized velocity and the stress field by the plane wave of the unit displacement amplitude respectively.

For an immersion ultrasonic pulse-echo measurement as shown in Fig. 1, substituting Eqs. (2)–(5) to Eq. (1), using the relation of the displacement amplitude with the velocity amplitude $\tilde{u}_j(\mathbf{x},\omega) = \tilde{v}_j(\mathbf{x},\omega)/(-i\omega)$ and rearrange the equation [12], the received signal for an immersed pulse-echo setup ($m = \alpha, v_T = v_R = v_o$), can be written as [1]:

$$V_R(\omega) = s(\omega)\left[\frac{4\pi\rho c_\alpha}{-ik_\alpha \rho_f c_f}\right] \int_S V^\alpha(\mathbf{x},\omega)^2 A(\mathbf{x},\omega) dS, \tag{6}$$

where $\mathrm{A}(\mathbf{x},\omega) = \frac{1}{4\pi\rho c_\alpha^2}\left(\tilde{\tau}_{ij} d_{Ij}^\alpha n_i + ik_\alpha C_{ijkl} d_{Sk}^\alpha e_{Sl}^\alpha \tilde{u}_j n_i\right)\exp(-ik_\alpha \mathbf{e}_S^\alpha \cdot \mathbf{x})$.

The term ρ_f and c_f represent the density and the sound speed of the fluid. In the expression A, to distinguish the incident wave and scattering wave, an "S" is added to the subscript of e and d to represent the scattering wave and "I" is added as the subscript to represent the incident wave. The unit vector $\mathbf{e}_S^\alpha$ represents a unit vector in the direction of a scattered wave in the solid, while e_{Sl}^α is the component of the unit vector $\mathbf{e}_S^\alpha$ in the scattered wave direction. The polarization of the incident wave and scattered wave are denoted as d_{Ij}^α and d_{Sk}^α, respectively.

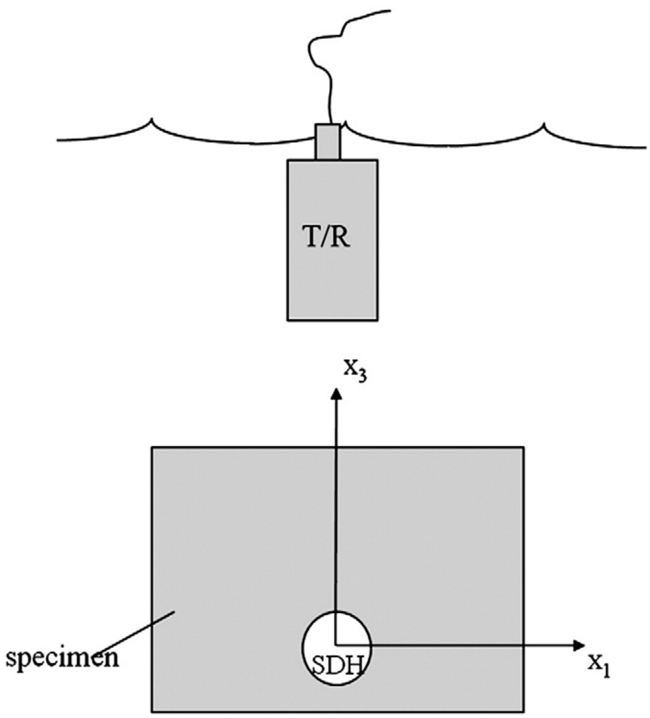

Fig. 1. An immersion ultrasonic pulse-echo measurement of the scattering from an SDH.

If the SDH is small enough to ignore the variation of the velocity fields over its cross-sectional area, which means that over the 'lit' surface of the cylinder the velocity fields is dependent of the x_2-coordinate along the cylinder, then Eq. (6) becomes [12]

$$V_R(\omega) = s(\omega)\left[\frac{4\pi\rho c_\alpha}{-ik_\alpha\rho_f c_f}\right]\int_L V^\alpha(\mathbf{x},\omega)^2 dx_2 \int_C A(\mathbf{x},\omega)dc(\mathbf{x}), \tag{7}$$

where c stands for the circumference of the SDH.

The far field scattering amplitude of the cylindrical reflector is given by

$$A_{3D}(\omega) = L\int_C A(\mathbf{x},\omega)dc(\mathbf{x}). \tag{8}$$

With Eqs. (8), (7) can be written as

$$V_R(\omega) = s(\omega)\left[\frac{4\pi\rho c_\alpha}{-ik_\alpha\rho_f c_f}\right]\int_L V^\alpha(\mathbf{x},s)^2 dx_2 \frac{A_{3D}(\omega)}{L}. \tag{9}$$

And there is a relationship between the two dimensional scattering amplitude and the three dimensional scattering amplitude, which can be expressed as [12]:

$$A_{3D}(\omega) = A_{2D}(\omega)L\left(\frac{k_\alpha}{2i\pi}\right)^{1/2}. \tag{10}$$

Therefore, the ultrasonic measurement model for the SDH can be expressed using the two-dimensional far-field scattering amplitude.

2.2. Kirchhoff approximation of the far-field pulse-echo scattering of an SDH in the anisotropic material

First, let us consider the problem of an SDH of radius r and length L contained in a three-dimensional, homogeneous, anisotropic and infinite elastic space, subjected to a plane qP-wave incident field, as shown in Fig. 2. The cylindrical coordinate system is chosen to have the x_2 direction coincident with the axis of the cylinder. The incident wave is assumed to be a plane wave, traveling in the negative x_3 direction.

From Eqs. (6), (8), and (10), the two dimensional scattering amplitude of the SDH in a pulse-echo setup can be written as follows, where C is the arc length [6]:

$$A_{2D}(\omega) = \sqrt{\frac{i}{8\pi k_\alpha}}\frac{1}{\rho c_\alpha^2}\int_C\left(\tilde{\tau}_{ij}d^\alpha_{lj}n_i + \frac{C_{ijkl}}{c_\alpha}d^\alpha_{Sk}e^\alpha_{Sl}\tilde{u}_j n_i\right)\exp(-ik_\alpha\mathbf{e}^\alpha_S\cdot\mathbf{x})dc(\mathbf{x}). \tag{11}$$

Since the distribution of scattered waves depends on the geometric and material properties of the flaw, it is necessary to solve an appropriate boundary value problem. However, at high frequencies, the Kirchhoff approximation can be applicable. This

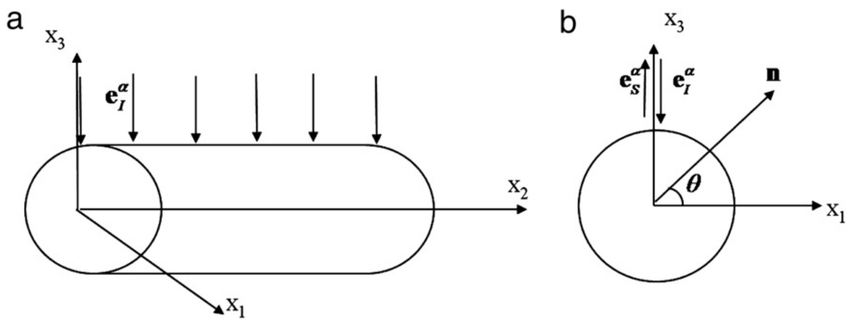

Fig. 2. (a) The pulse-echo scattering of an SDH of radius r and length L. The incident wave direction $\mathbf{e}_I^\alpha$, is assumed to lie in a plane perpendicular to the axis of the cylinder; and (b) the cross-section area of the SDH.

approximation assumes the shadow side of the scatterer to be motionless, while the lit side to move locally as if it were a planar surface lit by a plane wave with an amplitude equal to that of the local illuminating radiation. For the flaw is stress-free, $\tilde{\tau}_{ij} d_{Ij}^{\alpha} n_i = 0$, Eq. (11) can be reduced to

$$A_{2D}(\omega) = \sqrt{\frac{i}{8\pi k_\alpha}} \frac{1}{\rho c_\alpha^2} \int_{C_{lit}} \left(ik_\alpha C_{ijkl} d_{Sk}^{\alpha} e_{Sl}^{\alpha} \tilde{u}_j n_i \right) \exp(-ik_\alpha \mathbf{e}_S^{\alpha} \cdot \mathbf{x}) dc(\mathbf{x}). \tag{12}$$

On the lit surface, the total normalized displacement field can be expressed as the summation of the incident wave field and the reflected wave field [6]:

$$\tilde{u}_j = u_p^{inc} + u_p^{reflt} = d_{Ij}^{\alpha} \exp\left[ik_\alpha \left(\mathbf{e}_I^{\alpha} \cdot \mathbf{x}\right)\right] + \sum_{m = qP, qSV, qSH} R_{12}^{m;\alpha} d_{Rj}^{m} \exp\left[ik_\alpha \left(\mathbf{e}_I^{\alpha} \cdot \mathbf{x}\right)\right], \tag{13}$$

where $R_{12}^{m;\alpha}$ is the reflection coefficient at the interface for a reflected wave of type m due to an incident wave of type α. When it is a pulse-echo setup, the substitution of Eq. (12) with $\mathbf{e}_S^{\alpha} = \mathbf{e}_R^{\alpha} = -\mathbf{e}_I^{\alpha}$ and $d_R^{\alpha} = -d_I^{\alpha}$ leads to the following equation:

$$A_{2D}(\omega) = \sqrt{\frac{i}{8\pi k_\alpha}} \frac{1}{\rho c_\alpha^2} \int_{C_{lit}} \left(ik_\alpha C_{ijkl} d_{Ik}^{\alpha} D_p^{\alpha} e_{Il}^{\alpha} n_i \right) \exp\left[i2k_\alpha \mathbf{e}_I^{\alpha} \cdot \mathbf{x}\right] dc(\mathbf{x}) \tag{14}$$

where

$$D_p^{\alpha} = d_{Ij}^{\alpha} - \sum_{m = qP, qSV, qSH} R_{12}^{m;\alpha} d_{Ij}^{m}. \tag{15}$$

If one only considers the reflected qP-waves while the incident wave is the qP-waves, and multiply both sides of the Christoffel's equation $C_{ijkl} e_{Ij} e_{Il} d_{Ik} = d_{Ii} \rho c^2$ by $e_{Ij} d_{Ii}$, and substitute it into the part of the integrand of Eq. (15), one can get

$$C_{ijkl} d_{Ik}^{qP} D_p^{qP} e_{Il}^{qP} n_i = \rho c^2 n_i e_{Ij} \left(1 - R_{12}^{qP;qP}\right). \tag{16}$$

For $n_i e_{Ij} = \mathbf{e}_I^{\alpha} \cdot \mathbf{n} = \cos\left(\frac{\pi}{2} + \theta\right) = -\sin\theta$, Eq. (16) becomes

$$C_{ijkl} d_{Ik}^{qP} D_p^{qP} e_{Il}^{qP} n_i = \rho c^2 \left(1 - R_{12}^{qP;qP}\right)(-\sin\theta), \tag{17}$$

and

$$\mathbf{e}_I^{\alpha} \cdot \mathbf{x} = r\cos\left(\theta + \frac{\pi}{2}\right) = -r\sin\theta. \tag{18}$$

Substituting Eqs. (17), (18), and $dS = rd\theta$ for Eq. (14), it gives

$$A_{2D}(\omega) = \sqrt{\frac{i}{8\pi k_\alpha}} ik_\alpha \int_0^{\pi} \left[1 - R_{12}^{qP;qP}(\theta)\right] (-\sin\theta) \exp[-2ik_\alpha r \sin\theta] r d\theta \tag{19}$$

By the above procedure, a general integral form of a far-field scattering by an SDH in general anisotropic media is derived, however, obtaining an explicit analytic result of Eq. (19) is difficult due to complex interactions. Furthermore, for many applications, a general integral wave solution to the field is too difficult and time consuming, so employing one of the various approximations is often adequate and much quicker. The stationary phase method is an approximation method that takes advantage of the rapidly varying integrand's phase [6,16]. The solution to the integral is given by the contribution of certain points distributed over the surface of the body. Physically, the contributions resemble in the same way the typical contribution points in the traditional asymptotic techniques such as geometrical optics and geometrical theory of diffraction/uniform theory of diffraction (GO/UTD) [17]. The contributions are also called the leading edge response of the flaw [6]. From a ray point of view, the integral approximated by an asymptotic expansion around points where the phase is stationary states that energy travels primarily in straight lines from the source to the field point along ray paths that are normal to the slowness surface. In a wave interpretation, the stationary phase method picks out the plane wave with the slowest varying phase at each point, assuming the destructive interference of the others [16]. This approximation works in most cases, however, the phase may have, for example, more than one extrema, saddle points, and inflections then this approximation fails. Even though, it is possible to rewrite the asymptotic expansion in a piecewise fashion to handle these situations [6]. And it is currently being extended using the rather well-known uniform asymptotic expansion along with boundary layers [18], with excellent results for particular geometries.

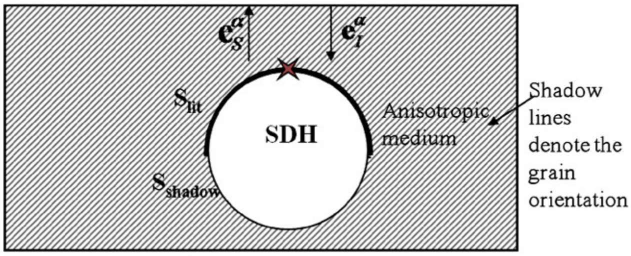

Fig. 3. The surface region of the SDH's circumference considered in the Kirchhoff approximation with the general integral (bold line) and with the stationary phase method (star).

Fig. 3 illustrates the region (or the point) of the SDH's circumference considered in the Kirchhoff approximations with the general integral and the stationary phase methods.

To evaluate Eq. (19), we want to compute the stationary values of the surface scattering integral of the type

$$A_{2D}(\omega) = \sqrt{\frac{i}{8\pi k_\alpha}} ik_\alpha \int_0^\pi f(\theta)\exp[ik_\alpha\varphi(\theta)]d\theta, \tag{20}$$

with defining $f(\theta) = (1 - R_{12}^{qP;qP}(\theta))(-\sin\theta)r$ and phase function $\varphi(\theta) = -2r\sin\theta$.

For at high frequencies, it is clear that $f(\theta)$ is a relatively slowly varying function of θ, whereas the $\exp[ik_\alpha\varphi(\theta)]$ is generally large and rapidly varying. The rapid oscillations of $\exp[ik_\alpha\varphi(\theta)]$ over most of the range of integration means that the integrand averages to almost zero [6].

In the stationary phase method, points θ_s of the stationary phase satisfy $\frac{\partial\varphi}{\partial\theta} = 0$, so only one stationary phase point: $\theta_s = \frac{\pi}{2}$. Note $\varphi(\theta_s) = -2r$, $\varphi''(\theta_s) = 2r$ and odd order derivatives are zero, so the resulting equation becomes

$$A_{2D}(\omega) = ik_\alpha\sqrt{\frac{i}{8\pi k_\alpha}}\sqrt{\frac{2\pi}{k_\alpha|\varphi''(\theta_s)|}}f(\theta_s)\exp[ik_\alpha\varphi(\theta_s) + i\pi\,\mathrm{sgn}\{\varphi''(\theta_s)\}/4] = -\sqrt{\frac{r}{8}}(i)^{\frac{3}{2}}\left[1-R_{12}\left(\frac{\pi}{2}\right)\right]\exp[-ik_\alpha 2r + i\pi/4]. \tag{21}$$

Substituting Eq. (21) into Eq. (10), the three dimensional scattering amplitude of the SDH in the anisotropic media is

$$A_{3D}(\omega) = \frac{L}{4}\sqrt{\frac{k_\alpha r}{\pi}}(1-R_{12})\exp[-i(k_\alpha 2r-3\pi/4)]. \tag{22}$$

Eq. (22) is our final, three dimensional far-field scattering amplitude of the SDH in a pulse-echo setup using stationary phased method. Compared to Eq. (19), the stationary phase method provides a fourth order accurate of the phase function. Compared to the stationary phase method as Eq. (21) to the general integral form as Eq. (19), an asymptotic error occurs when the reflection coefficient is not symmetric with respect to the normal to the interface, that is, the oscillations of the integrand cannot be canceled.

For the isotropic media, $R_{12}^{qP;qP} = -1$, so Eq. (22) can be simplified to

$$A_{3D}(\omega) = \frac{L}{2}\sqrt{\frac{k_\alpha r}{\pi}}\exp[-i(k_\alpha 2r-3\pi/4)]. \tag{23}$$

If we compare Eq. (18) with the expression in the isotropic case in Ref. 12, we see that both expressions are the same. However, the reflection coefficient of the anisotropic material in Eq. (22) is much more complex than that of the isotropic one. It depends on the incident angle and stiffness tensor as well. The complication of the problem also arises from the variation of the slowness with the direction of the propagation. In the anisotropic medium, the incident, reflected plane waves do not have in general purely longitudinal or transverse polarizations. Even so, when solving the Christoffel's equation, the three polarizations of the reflected plane waves are found still mutually orthogonal to each other. In the following, reflection coefficients for the anisotropic materials and void SDH will be derived.

2.3. Reflection coefficients

To solve the problem of determining the reflection coefficients of a plane wave with an incident wave propagating in the negative x_3 direction on an SDH interface between an anisotropic half space and a void as shown in Fig. 2, we can consider the problem as the same one as to determine the reflection coefficients for plane waves travelling in arbitrary directions relative to a traction-free scattering surface [13,19,20].

We let s^I be the incident slowness vector, $s^{R,qP}$,$s^{R,qSV}$,$s^{R,qSH}$ be the three reflected slowness vectors, respectively. Then the incident and reflected waves can be expressed as

$$s^{I,R} = \frac{k}{\omega}\mathbf{e}^{I,R}. \tag{24}$$

For the interface between the anisotropic media and a void, it is a free boundary problem, so the stresses vanish

$$\begin{aligned} &\sigma_{13}^{I} + \sum_{m=qP,qSV,qSH} \sigma_{13}^{R,m} = 0, \\ &\sigma_{23}^{I} + \sum_{m=qP,qSV,qSH} \sigma_{23}^{R,m} = 0, \\ &\sigma_{33}^{I} + \sum_{m=qP,qSV,qSH} \sigma_{33}^{R,m} = 0. \end{aligned} \tag{25}$$

To determinate the σ_{i3} components in the anisotropic media, we first express the displacements as

$$u_i^m = U^m d_i^m e^{i(k_n x_n - \omega t)}, \tag{26}$$

then the stress–strain equation for the solid as

$$\sigma_{ij}^m = C_{ijkl}\varepsilon_{kl}^m, \tag{27}$$

and the strain–displacement relation as

$$\varepsilon_{kl}^m = \frac{1}{2}\left(\frac{\partial u_k^m}{\partial x_l} + \frac{\partial u_l^m}{\partial x_k}\right). \tag{28}$$

Using the displacement given in Eq. (26) then we can express the stress components as

$$\sigma_{i3}^m = i\omega C_{i3kl}s_k^m d_l^m U^m. \tag{29}$$

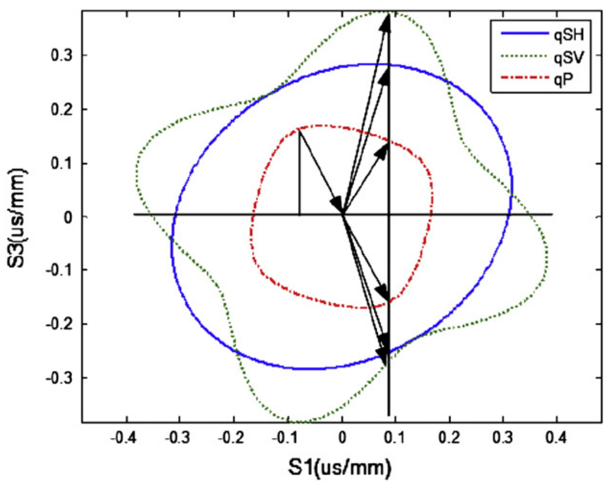

Fig. 4. Six solutions for a given incident angle of austenite steel [21].

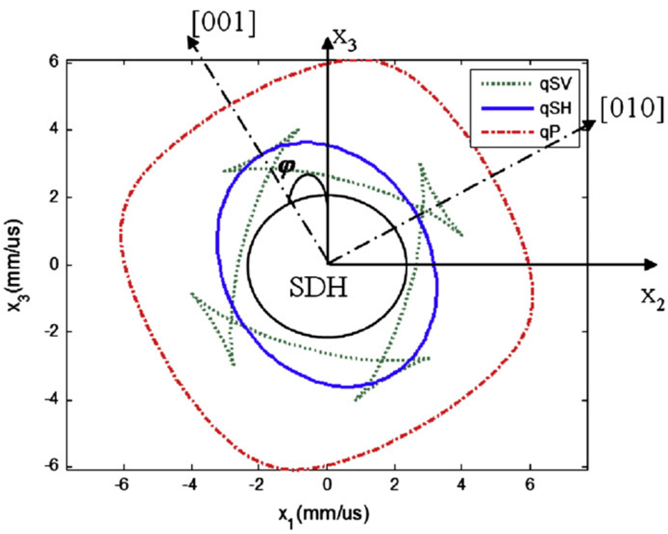

Fig. 5. Three group velocities of austenite steel in the incidence plane (100) with a rotation angle φ.

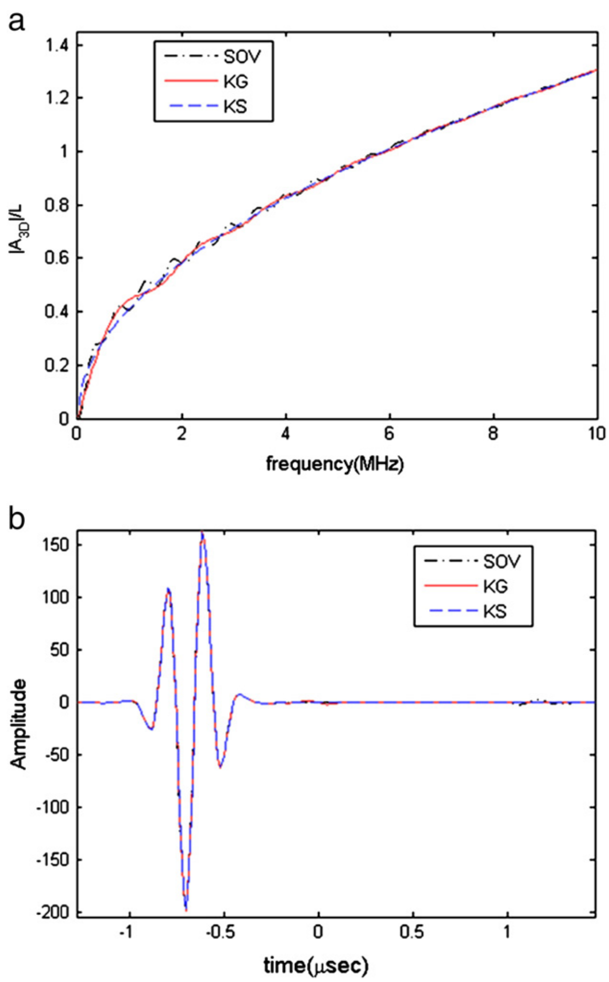

Fig. 6. The three-dimensional normalized pulse-echo qP-wave scattering amplitude versus the frequency for an SDH in the Kirchhoff approximation using the stationary phased method (blue dash line), general integral method (red solid line) and the separation of variables solution (black dash–dot line).

With defining a quantity $D_i^m = C_{i3kl}s_k^m d_l^m$, D_i^m can be given explicitly in terms of the reduced stiffness components as

$$\begin{aligned}
D_1^m &= (s_1^m C_{15} + s_3^m C_{55})d_1^m + (s_1^m C_{56} + s_3^m C_{45})d_2^m + (s_1^m C_{55} + s_3^m C_{35})d_3^m, \\
D_2^m &= (s_1^m C_{14} + s_3^m C_{45})d_1^m + (s_1^m C_{46} + s_3^m C_{44})d_2^m + (s_1^m C_{45} + s_3^m C_{34})d_3^m, \\
D_3^m &= (s_1^m C_{13} + s_3^m C_{35})d_1^m + (s_1^m C_{36} + s_3^m C_{34})d_2^m + (s_1^m C_{35} + s_3^m C_{33})d_3^m.
\end{aligned} \tag{30}$$

Introducing a reflection coefficient

$$R = U^m / U^\alpha, \tag{31}$$

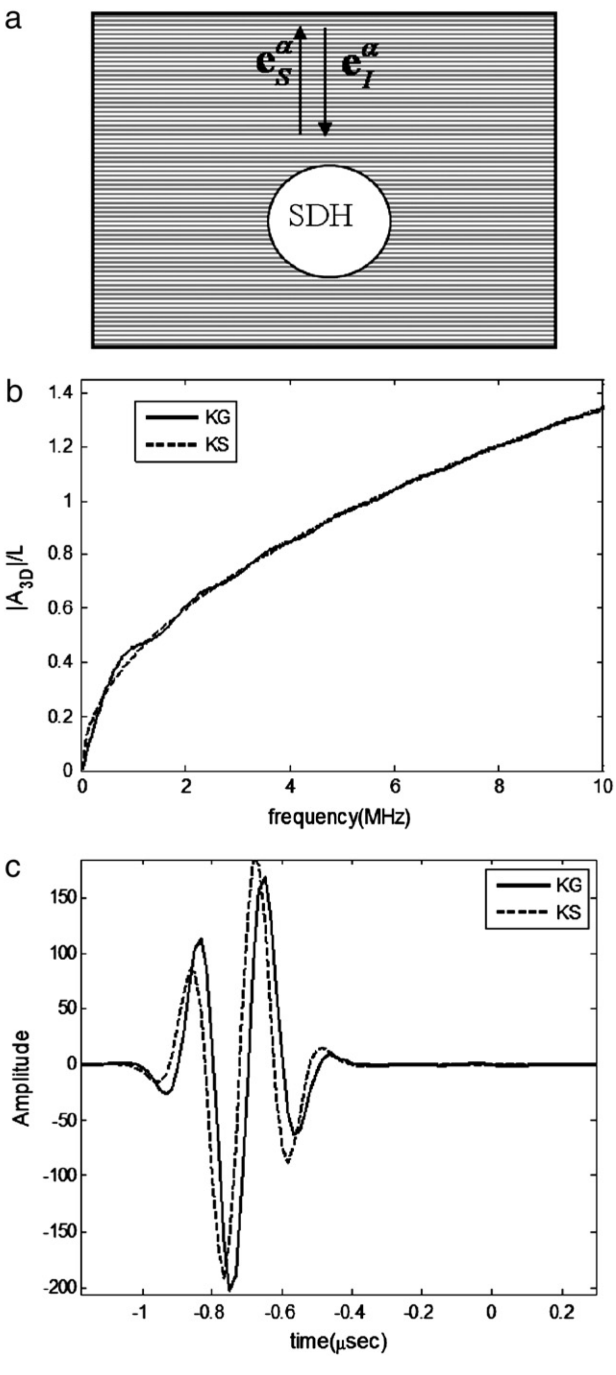

Fig. 7. (a) The pulse-echo case where $\mathbf{e}_i$ is normal to the grain orientation direction [010] ($\varphi = 0°$), (b) the normalized pulse-echo qP-wave scattering amplitude versus the frequency, and (c) the time domain wave form for an SDH in the KS (dash line) and KG (solid line).

then we can have the following matrix equation

$$\begin{pmatrix} D_1^{qP} & D_1^{qS_1} & D_1^{qS_2} \\ D_2^{qP} & D_2^{qS_1} & D_2^{qS_2} \\ D_3^{qP} & D_3^{qS_1} & D_3^{qS_2} \end{pmatrix} \begin{pmatrix} R^{qP} \\ R^{qS_1} \\ R^{qS_2} \end{pmatrix} = -\begin{pmatrix} D_1^{\alpha} \\ D_2^{\alpha} \\ D_3^{\alpha} \end{pmatrix}. \tag{32}$$

Solving Eq. (32) yields the reflection coefficients which are needed in the SDH scattering problem in an anisotropic material.

To evaluate Eq. (32) the polarizations d_l^m and the slowness vector values have to be found. For the harmonic plane waves, all the slowness vectors lie in the same incident plane and have the same projection onto the boundary as the incident wave (which is

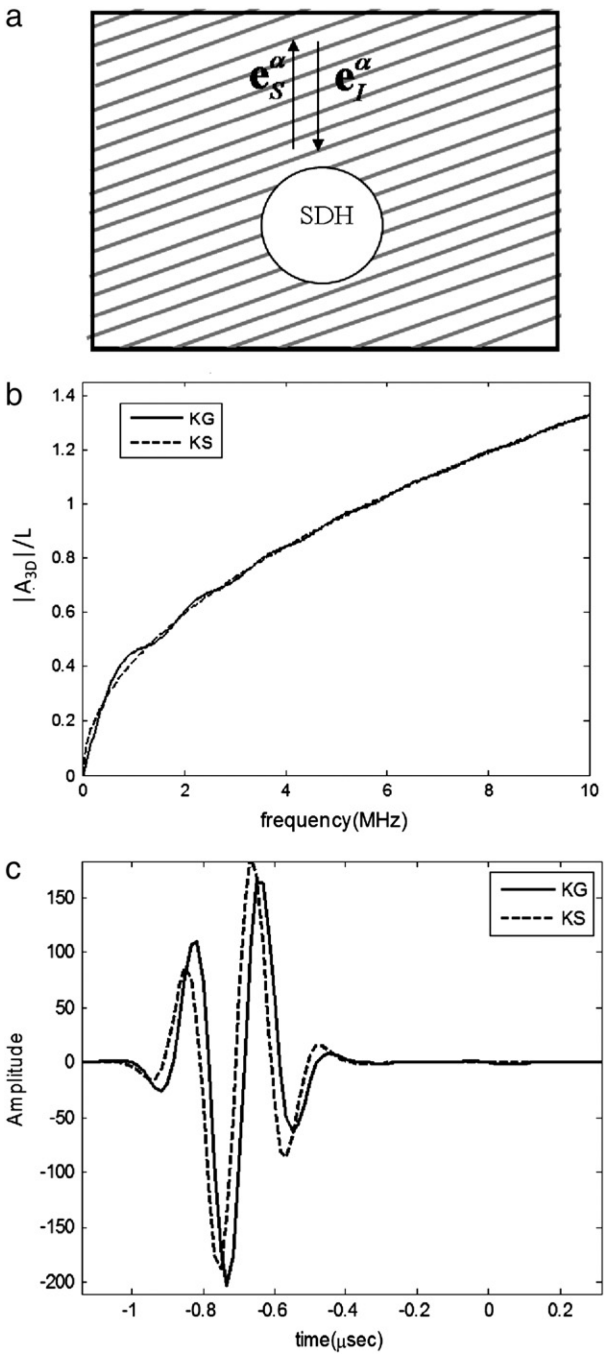

Fig. 8. (a) The pulse-echo case where the angle between $\mathbf{e}_i$ and the normal to the grain orientation direction [010] is 30° ($\varphi = 30°$), (b) the normalized pulse-echo qP-wave scattering amplitude versus the frequency, and (c) the time domain wave form for an SDH in the KS (dash line) and the KG (solid line).

acquired by Snell's law). Thus, if the interface coordinate system is selected the slowness components for the reflected and refracted waves s_2^α is zero, and s_1^α is equal to the incident slowness component which is known, then only the slowness component which is left to be determined is s_3^α. To determine the s_3^α the Christoffel's equation needs to be set as follows [20],

$$\left(C_{ijkl}s_js_k - \rho\delta_{il}\right)d_l = 0, \tag{33}$$

The determinant of the coefficients, when the set equals to zero, determines the three sheets of the slowness surface, which can be expanded to a sixth order equation for s_3^α since $s_2 = 0$ and s_1^α is known. For a given s_1^α, six solutions can be found in the anisotropic medium as shown in Fig. 4.

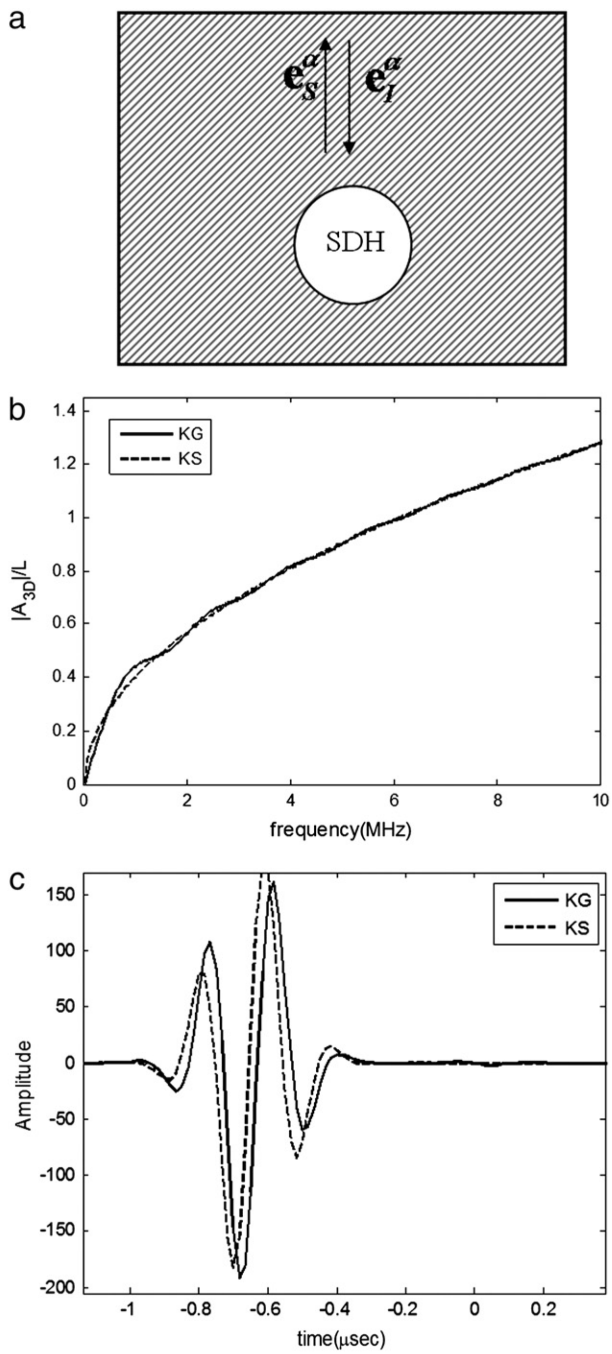

Fig. 9. (a) The pulse-echo case where the angle between $\mathbf{e}_i$ and the normal to the grain orientation direction [010] is 45° ($\varphi = 45°$), (b) the normalized pulse-echo qP-wave scattering amplitude versus the frequency, and (c) the time domain wave form for an SDH in the KS (dash line) and the KG (solid line).

In the anisotropic media, the selection of the transmitted waves is based on the energy flow direction, also called the direction of the group velocity vector. The group velocity is determined mathematically by [22]

$$g_j = \frac{1}{\rho} C_{ijkl} s_k d_l d_i \tag{34}$$

Thus we must select such reflected root for which group velocity vector points back to the first medium, that is the scalar product of the normal to the plane interface and the propagation direction should be bigger than zero. This criterion solves the problem completely, if all six roots are real-valued. An even number of roots, however, may be complex-valued (pairs of complex–conjugate roots). Only one physical root of any pair of complex–conjugate roots should be selected. The proper wave should be with amplitudes decreasing exponentially with increasing distance from the interface to the second half space.

3. Numerical results and discussion

We shall illustrate the application of the analytical solution proposed in the present study and discuss the different features of the scattering waves from the SDH in the anisotropic material for some selected cases.

First, we take an anisotropic material: austenitic stainless steel, which is transversely isotropic. This material is chosen because it is a common filler material in the weld. Its elastic constants and density are listed herein.

$$C_{ij} = \begin{pmatrix} 2.4110 & 0.9692 & 1.3803 & 0 & 0 & 0 \\ 0.9692 & 2.4110 & 1.3803 & & & \\ 1.3803 & 1.3803 & 2.4012 & & & \\ & & & 1.1229 & & \\ & & & & 1.1229 & \\ & & & & & 0.7209 \end{pmatrix} \times 10^9 \mathrm{N/m^2}$$

$$\rho = 7.82 \times 10^3 \mathrm{kg/m^3}$$

And the radius of the SDH is 2 mm, which is a common size in the ultrasonic benchmarking study [23].

The incident plane in which the incident wave and all the reflected waves lie can be selected arbitrarily. The scattering phenomena will be in the general case, even though the material is transversely isotropic. Thus the anisotropic medium selected previously will reflect the general behavior of an austenite crystal. In the anisotropic media, the Cartesian coordinate does not

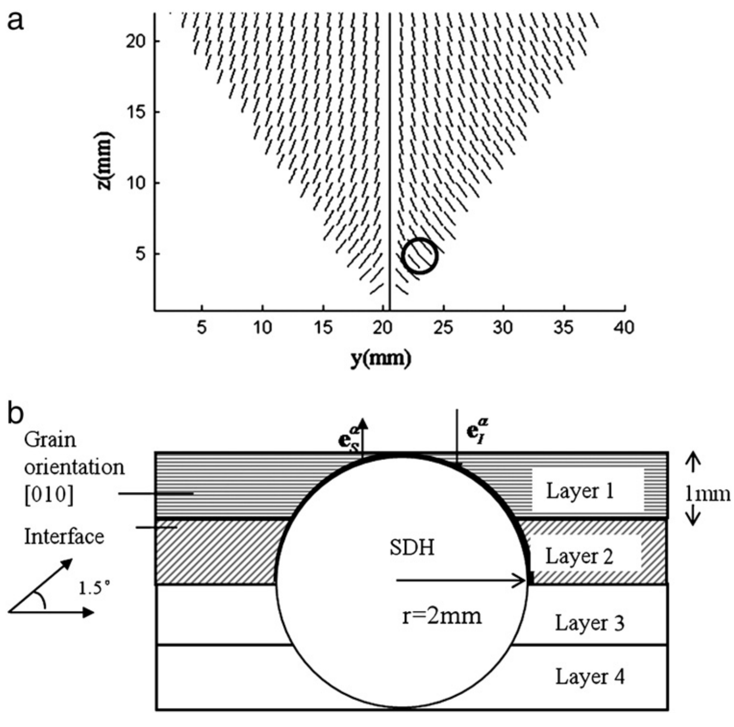

Fig. 10. (a) The grain orientation of the weld modeled by Ogilvy, (b) an SDH with $r = 2$ mm embedded in the layered structure.

always lie parallel to the crystal coordinate, thus a rotation angle φ is defined as shown in Fig. 5. Fig. 5 also indicates that the Cartesian coordinates whose axes are named x_1, x_2 and x_3, while the crystal coordinate whose axes are named [010], [100] and [001], planes are named (001) etc. according to the Miller index [24]. We illustrate the scattering problem by considering some particular incidence planes as well as some rotation angles. Since the physical behavior of transversely isotropic material in (010) plane is the same as that in (100) plane, plane (010) will not be discussed, but planes (100) and (001) are chosen as the incidence planes here.

First, let's consider the incidence plane (001). For the material is isotropic in this plane, the simulation results of the Kirchhoff approximation can be compared with the exact analytical result using the separation of variables [12].

Fig. 6(a) shows a comparison of the results obtained by three approaches: 1) the Kirchhoff approximation with the stationary phase method (hereafter 'KS' solution), 2) the Kirchhoff approximation with the general integral method (hereafter 'KG' solution), and 3) the separation of variables method (hereafter 'SOV' solution). From Fig. 6(a), one can notice that the KS and KG solutions match very well to the SOV solutions, except for some small oscillations which the SOV solution contains. Particularly, at the higher frequencies, the agreement among three solutions is even better. Generally, it is understood that the Kirchhoff approximation is not applicable when $kr < 1.5$ [12]. So in this case, when r is 2 mm, the simulation is not correct until the frequency is higher than 0.75 MHz. In fact, the oscillations appeared in the low frequencies are due to the creeping wave, but the Kirchhoff approximation cannot describe them precisely. Fig. 6(b) shows the corresponding time-domain pulse-echo qP-wave responses of the SDH void obtained by taking the inverse Fourier transform to the system function $s(\omega)$ with the center frequency of 5 MHz and the bandwidth of 4 MHz to the scattering amplitude presented in Fig. 6(a). In Fig. 6(b), the creeping waves can be observed on the waveforms of the SOV and the KG solutions.

In the incidence plane (100), the scattering behaviors for the rotation angles of 0°, 30° and 45° are evaluated, since the variation in the group velocity is relatively large around 45° while the variation is mild around 30°. Investigations will be focused on the validation of the Kirchhoff approximation results (i.e., the KG and KS solutions).

Figs. 7(b), 8(b), and 9(b) show the scattering amplitudes in the frequency domain with different rotation angles. By comparing these results, one can notice that the amplitude with $\varphi = 45°$ is smaller than the one with $\varphi = 30°$, while the one with $\varphi = 30°$ is smaller than $\varphi = 0°$. This result is accordance with Eq. (22), which shows A_{3D} is proportional to the square root of k_α, while k_α is

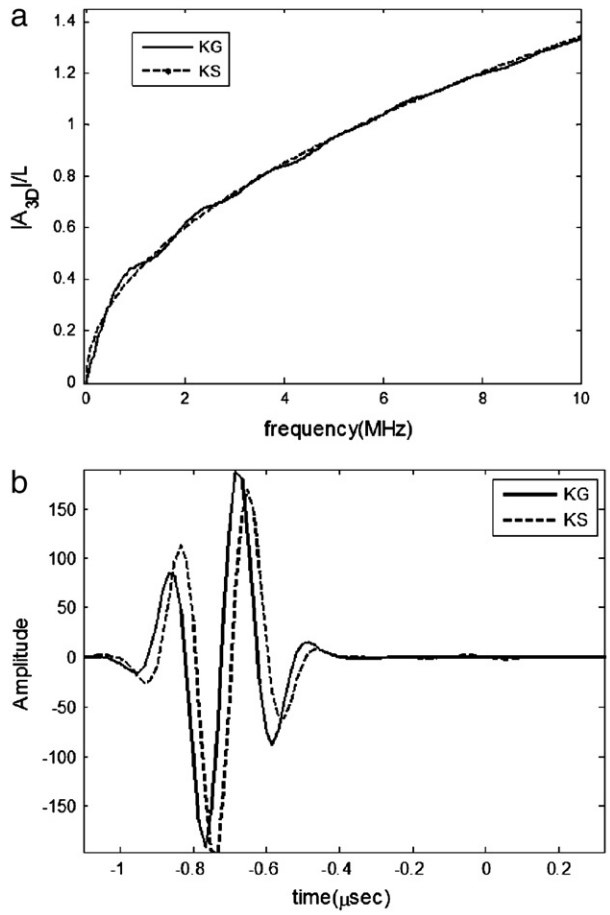

Fig. 11. The normalized pulse-echo qP-wave scattering amplitude versus the frequency and the time domain wave form for an SDH in the KS (dash line) and the KG (solid line) in layered anisotropic media model.

reciprocal to the group velocity. Fig. 5 shows that the group velocity decreases from $\varphi=45°$ to $\varphi=0°$ in incident plane (100) of austenite steel. In the case of $\varphi=0°$ and $\varphi=45°$ where the incident plane is symmetric with respect to the normal to the interface, one can also notice that except for some small oscillations, the KS solution matches well with the KG solution, particularly at higher frequencies in Figs. 7 and 9. While, the amplitude of the scattering of the SDH shown in Fig. 8 shows a little difference between the KG and the KS. The ignorance of the contribution of the non-stationary phased points from the asymmetry when the incident plane is asymmetric to the normal of the interface at $\varphi=30°$ accounts for the asymptotic error. However, the variation of the value of the group velocity of the qP wave in the austenite steel shown in Fig. 5 is between 5541 m/s and 6210 m/s, so the asymptotic error is acceptable. But when the variations of the group velocity are big, then the stationary phase method is not reliable compared to the general integral method.

Next, we are extending the application boundary of the Kirchhoff approximation to the weld which can be described as the multi-layered anisotropic materials, but with the slowly varying orientations from a layer to the neighboring layer [25,26]. The grain orientation of the weld modeled by Ogilvy's model is shown in Fig. 10(a), and an SDH with r = 2 mm embedded in the layered structure is shown in Fig. 10(b). By observation of the welds, the grain orientation between two neighboring layers is less than 1.5°, and the thickness of each layer is around 1 mm. Fig. 10 shows that the whole SDH occupies 4 layers, however the half of the circle only occupies 2 layers. So, two layers are sufficient for the investigation of the wave scattering from the SDH using the Kirchhoff approximation.

Fig. 11 is an example of the far-field scattering responses of an SDH in the two layered anisotropic media predicted by the KG and the KS methods. The two layers are both in the plane (010), and the layer 1 has a rotation angle of 0 ° while the layer 2 has 1.5°. The simulation results using the KG and KS methods in the two layered media are almost identical, especially in the high frequency part. Since the KG has no restrictions in the application in the Kirchhoff approximation, with taking all the lit points into account in the integral, the result of the KG can be considered as a reliable one. The high similarity between the results by the KG and the KS convinced us that the KS solution can be applied to the weld too, when the incident plane is not in a severe asymmetrical condition. The KS method is simpler to implement and calculates more efficiently.

4. Conclusion

The theoretical evaluation of the elastic wave scattering from an SDH in the anisotropic media has been addressed. The incident wave is assumed to be normal to the axis of the cylindrical hole. Using the Kirchhoff approximation, the far-field three dimensional scattering amplitude of the SDH has been derived. In introducing the stationary phase method, we have obtained the explicit expression of the scattering amplitude. The proposed analytical solutions have been evaluated numerically for various cases with different incident angles and grain orientations in the homogeneous anisotropic media. The figures show the numerical agreement of the obtained results with those calculated using the Kirchhoff approximation with the general integral method and with the separation of variables. We have also extended the application of the proposed solutions to the multi-layered anisotropic materials successfully. However, it is worthwhile to mention that the present analysis is restricted to the scattering problem only and it would be necessary to expand the analysis to include the velocity field amplitude to construct a complete ultrasonic measurement model as a further investigation.

Acknowledgement

This work was supported by the Korea Science and Engineering Foundation (KOSEF) grant funded by the Korea government (MOST) (No. 2006-01653).

References

[1] A.L. Lopez-Sanchez, H.J. Kim, L.W. Schmerr, Measurement models and scattering models for predicting the ultrasonic pulse-echo response from side-drilled holes, J. Nondestr. Eval. 24 (2005) 83–96.
[2] R.M. White, Elastic wave scattering at a cylindrical discontinuity in a solid, J. Acoust. Soc. Am. 30 (1958) 771–785.
[3] A.J. Niklasson, S.K. Datta, Scattering by an infinite transversely isotropic cylinder in a transversely isotropic medium, Wave Motion 27 (1998) 169–185.
[4] J. Krautkraemer, H. Krautkraemer, Ultrasonic Testing of Materials, fourth ed., Springer, Berlin, 1990.
[5] R.K. Chapman, A system approach for the ultrasonic inspection of smooth planar cracks, J. Nondestr. Eval. 9 (1990) 197–211.
[6] L.W. Schmerr, Fundamentals of Ultrasonic Nondestructive Evaluation: A Modelling Approach, Plenum, New York, 1998.
[7] A. Bostrom, P. Bovik, Ultrasonic scattering by a side-drilled hole, Int. J. Solids Struct. 40 (2003) 3493–3505.
[8] K. Harumi, M. Uchida, Computer simulation of ultrasonics and its applications, J. Nondestr. Eval. 9 (1990) 81–99.
[9] P. Fellinger, R. Marklein, K.J. Langenberg, S. Klaholz, Numerical modeling of elastic wave propagation and scattering with, EFIT—elastodynamic finite integration technique, Wave Motion 21 (1995) 47–66.
[10] D. Placko, KunduT. , DPSM for Modeling Engineering Problems, Wiley-Interscience, 2007.
[11] S. Das, S. Banerjee, T. Kundu, Elastic wave scattering in a solid half-space with a circular cylindrical hole using the distributed point source method, Int. J. Solids Struct. 45 (2008) 4498–4508.
[12] L.W. Schmerr, S.J. Song, Ultrasonic Nondestructive Evaluation Systems Models and Measurements, Springer, 2007.
[13] M. Spies, Kirchhoff evaluation of scattered elastic wavefields in anisotropic media, J. Acoust. Soc. Am. 107 (2000) 2755–2759.
[14] R.J. Huang, L.W. Schmerr, S. Alexander, T.A. Gray, Kirchhoff approximation revisited—some new results for scattering in isotropic and anisotropic elastic solids, Res. Nondestr. Eval. 17 (2006) 137–160.
[15] B.A. Auld, General electromechanical reciprocity relations applied to the calculation of elastic wave scattering coefficients, Wave Motion 1 (1979) 3–10.
[16] Brian O'Neill, Roman Gr. Maev, Mathematical methods for the characterization of ultrasound in anisotropic materials, Can. J. Phys. 78 (2000) 803–820.
[17] R.G. Kouyoumjiam, P.H. Pathak, A uniform geometrical theory of diffraction for an edge in a perfectly conducting surface, Proc. IEEE 62 (1974) 1448–1461.

[18] D. Gridin, L.J. Fradkin, The high-frequency asymptotic description of pulses radiated by a circular normal transducer into an elastic half-space, J. Acoust. Soc. Am. 104 (1998) 3190–3198.
[19] E.G. Henneke, Reflection–refraction of a stress wave at a plane boundary between anisotropic media, J. Acoust. Soc. Am. 51 (1972) 210–217.
[20] S.I. Rokhlin, T.K. Bolland, Laszto Addler, Reflection and refraction of elastic waves on a plane interface between two generally anisotropic media, J. Acoust. Soc. Am. 79 (1986) 906–918.
[21] Xinyu Zhao, Sung-Jin Song, Hak-Joon Kim, Tie Gang, Suk-Chull Kang, Yong Hwan Choi, Kyungcho Kim, Sung-Sik Kang, Determination of ultrasonic beam incident angle and position for flaw detection in anisotropic and inhomogeneous weldments by ray tracing, J. Korean Soc. Nondestructive Test. 27 (2007) 231–238.
[22] B. Mandal, Reflection and transmission properties of elastic waves on a plane interface for general anisotropic media, J. Acoust. Soc. Am. 90 (1991) 1106–1118.
[23] S.J. Song, L.W. Schmerr, R.B. Thompson, Ultrasonic benchmark study: overview up to year 2005, in: D.O. Thompson, D.E. Chimenti (Eds.), Review of Progress in QNDE, 25B, American Institute of Physics, Melville, N.Y, 2006, pp. 1844–1853.
[24] P. James, B. Bernard, Solid-State Physics: Introduction to the Theory, Springer, 2007.
[25] J.A. Ogilvy, A layered media model for ray propagation in anisotropic inhomogeneous materials, Appl. Math. Model. 14 (1990) 237–247.
[26] J. Ye, H.J. Kim, S.J. Song, M.H. Song, S.C. Kang, S.S. Kang, K.C. Kim, Determination of focal laws for ultrasonic phased array testing of dissimilar metal welds, J. Korean Soc. Nondestructive Test. 28 (2008) 247–435.